Edge-dislocation intersections in diamond cubic crystals

Mark Mostoller, M. F. Chisholm, and Theodore Kaplan
Solid State Division, Oak Ridge National Laboratory, Oak Ridge, Tennessee 37831
(Received 2 May 1994)

Results are presented for the atomic structure and energetics of possible intersections of (necessarily) orthogonal $(a/2)\langle 110\rangle$ edge dislocations in Ge/Si bicrystals, as predicted by classical simulations. The most compact structure is found to be preferred energetically.

I. INTRODUCTION

In a previous paper,[1] we predicted that a new defect structure would occur at the intersection of orthogonal $(a/2)\langle 110\rangle$ edge dislocations in Ge/Si(001) bicrystals. There is a 4% lattice mismatch between Si ($a=5.431$ Å) and Ge ($a=5.657$ Å) which can be relieved by the formation of a square grid of these dislocations at the interface,[2] with a spacing on the grid of 96 Å. Using classical numerical simulations, we found a defect structure at the intersections that was closed and symmetric, and contained 18 atoms. We call this structure the dreidl after the child's top that it evokes.[3]

The dislocations with Burgers vectors $(a/2)[1,\pm 1,0]$ that intersect to form the dreidel are offset from one another by one layer along $z=[0,0,1]$. Larger offsets of 3,5,7, . . . , layers are also possible (an explanation of why only odd numbered spacings are allowed will be given later). Since the defect structure spans seven layers, three- and five-layer offsets should also lead to intersections, while a seven-layer offset is the minimum for which no intersection occurs. In Ref. 1, we considered only one possible intersection, the one that is the most compact, has the minimum offset and was predicted by the simulations of the mismatched Ge film and Si substrate. In other situations, however, other intersections may occur, and it is important to investigate their structures and energies. Intersections will impact the motion of dislocations, and serve as pinning centers that influence the strength and strain hardening of materials. In this paper, the structures found for the different intersections are shown, and their relative energies (including the case of no intersection) are discussed. Section II describes the simulations, and Sec. III presents the results.

II. SIMULATIONS

The grid of dislocations forms to accommodate the mismatch between the Si substrate and the growing Ge film. This growth process takes place on a time scale that is not amenable to atomistic simulation, so a combination of simulated annealing and total-energy minimization was used to study the structures that might form. As a first step in constructing starting samples, crystals of Ge and Si were created, each having 16 layers along $z=[0,0,1]$; the Ge crystal had 24 layers along $x=[1,-1,0]/\sqrt{2}$ and $y=[1,1,0]/\sqrt{2}$, and the Si crystal had 25 layers along these directions corresponding to the 4% lattice mismatch. The Ge crystal was then placed on top of the Si crystal.

We digress briefly to discuss constraints imposed by the crystal structure. Figure 1 shows the structure of isolated $(a/2)\langle 110\rangle$ edge dislocations in diamond cubic

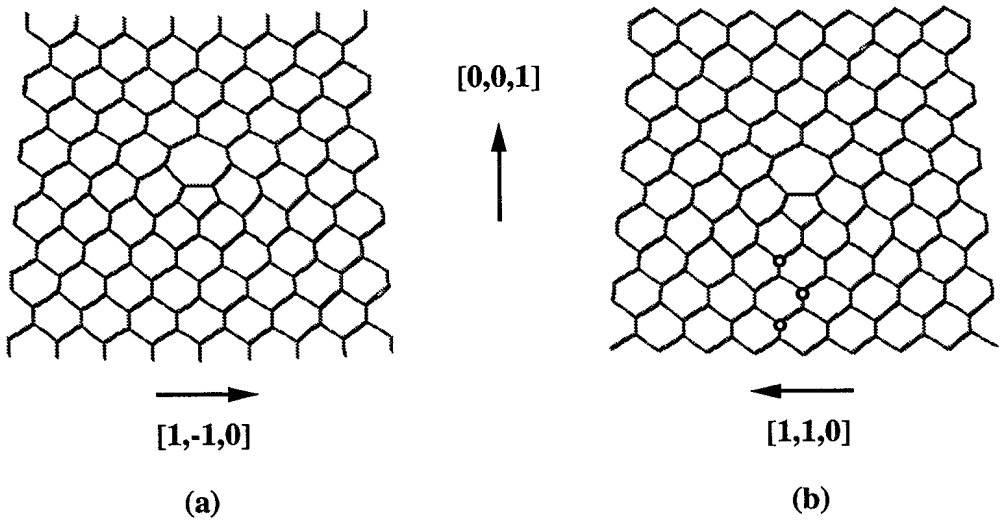

FIG. 1. Projections of edge dislocations along $y=[1,1,0]$ and $x=[1,\bar{1},0]$ in diamond cubic crystals. In the x projection (b), allowed positions for the bottom of the pentagon are marked.

0163-1829/94/50(16)/12183(4)/$06.00

crystals. At the core there appear the familiar linked fivefold plus sevenfold rings, with every atom retaining tetrahedral bonding.[4,5] In Fig. 1(a), the dislocation line runs perpendicular to the plane of the figure along $y=[1,1,0]$. Note that the atoms at the top of the heptagon and the bottom of the pentagon in this projection are joined by vertical "double bonds" to the next layers above and below, respectively. Notice also that the very top two and bottom two layers of the section of crystal shown are connected by double bonds. Figure 1(b) shows a dislocation along the $x=[1,-1,0]$ direction. The atoms in the top and bottom layers of this sample form single bonds to the adjacent layers shown, and careful inspection will persuade the reader that the dislocation has moved downward by one layer compared to Fig. 1(a). It must do this to satisfy the requirement that the atoms at the top of the heptagon and the bottom of the pentagon have the correct bonding to the layers above and below, respectively.

If we want to move one of the dislocations in Fig. 1 down relative to the other, the crystal structure requires that we move it downward by an even number of layers along a zigzag path. The allowed locations for the bottom of the pentagon along such a zigzag path are marked in Fig. 1(b). We thus get offsets of 1,3,5,7,..., layers between the orthogonal dislocations. Even layer offsets are not allowed. For 1-, 3-, and 5-layer offsets, the dislocations will intersect, while for offsets of 7, 9, . . . , they will not. In the starting sample of Ge stacked on Si as we have constructed it, a central column of atoms along x must be removed in the top layer of Si to satisfy the stacking constraints set by the crystal structure. The dislocation that forms along x can be moved downward into the Si half of the bicrystal by removing successive pairs of columns of atoms in the starting sample in the zigzag pattern shown in Fig. 1(b).

Because of the lattice mismatch between Si and Ge, there are extremely large forces present at the interface of the stacked starting sample. The Ge and Si atoms are in perfect registry for tetrahedral bonding across the interface at the corners of the periodic repeat boundaries along x and y, and are out of registry at the center. To facilitate the simulations, some prehealing was done to reduce these very large forces. The Ge atoms in the first half plane at the interface were healed away from the center where the individual dislocations will form. In the final results, the atomic positions are bowed downward in the center along z by substantial amounts as a consequence of the strains introduced by the dislocation array. Accordingly, the atoms in the Si half of the starting sample were bowed downward at the outset to reduce the initial forces.

In the simulations, periodic boundary conditions were applied along the x and y directions, with free surfaces along $z=[0,0,1]$. The Si and Ge (001) surfaces reconstruct by dimerizing of $\langle 110 \rangle$ rows. With starting samples prepared as set forth above, annealing and minimization produces a random dimerization of the top and bottom surfaces that makes it impossible to compare the energies of the different intersections. The final step in constructing the starting samples was therefore to regularly dimerize the top and bottom layers, and to monitor this from start to finish of the simulations.

The procedure outlined gave four starting samples with 19 191–19 041 atoms for the various intersections—19 191 for the dreidl, the most compact intersection, to 19 041 for no intersection. Each sample had 9216 Ge atoms; the number of Si atoms varied in steps of 50 along the sequence 9975, 9925, 9875, 9825. The calculations done to find intersection structures and energies were kept as similar as possible once a successful path was found. Because the starting samples still had very large initial forces, they were first annealed at very low T, removing energy every time step and then every few time steps. The crystals were then raised briefly to rather high temperatures of $T \sim T_M/2$, where T_M is the melting temperature of Si, and annealed slowly back down to low T. Finally, the total energy was minimized at $T=0$. The first series of simulations was done with the Stillinger-Weber (SW) potential[6–8] because of its greater interaction range. To obtain energies with the Tersoff potential,[9] the atom positions found with the SW potential were raised to room temperature, annealed quickly, and minimized. All calculations were done at constant volume in order to maintain the proper periodicity in the xy plane.

III. RESULTS

Simulations were done for four cases which we will refer to as intersections 1–4, from the most compact intersection (intersection 1, the dreidl) to the first nonintersection (4). The structures predicted for intersections 1–3 are shown in Fig. 2. The dreidl contains 18 atoms, intersection 2 has 24, and intersection 3 contains 27. In intersection 3, the cores of the orthogonal dislocations share only the single atom at the top of one and the bottom of the other.

To produce the various intersections, we removed 1, 3, 5, and 7 central columns of Si atoms in the starting bicrystal. As a consequence, the number of Si atoms in the samples decreases in steps of 50 from 9975 to 9825. The number of Ge atoms remains constant at 9216 for 16 layers of 576 atoms each. Table I gives results for the four relaxed samples with differing numbers of atoms for the two potentials. Average energies per atom $\langle E(\mathrm{Ge,Si}) \rangle$ are determined from all of the tetrahedrally coordinated atoms in the bicrystals, that is, from all atoms except those in the bottom Si and top Ge layers. As the intersection stretches downward into the Si substrate, $\langle E(\mathrm{Ge}) \rangle$ decreases slightly and $\langle E(\mathrm{Si}) \rangle$ increases by larger amounts. The cohesive energy $-V$ decreases by about 230 eV in each step with the SW potential and almost 250 eV with Tersoff, but this is not a fair comparison of the energies of the different intersections because the number of atoms is not constant.

To assess the relative energies of the various intersections, we do the following. Global average energies $\langle\langle E(\mathrm{Ge,Si}) \rangle\rangle$ are found by averaging over the four samples for each potential (see Table I for values). Total energies $V(\mathrm{Si})$ for "standard" samples with the same number of Si atoms as for intersection 1 are then obtained by

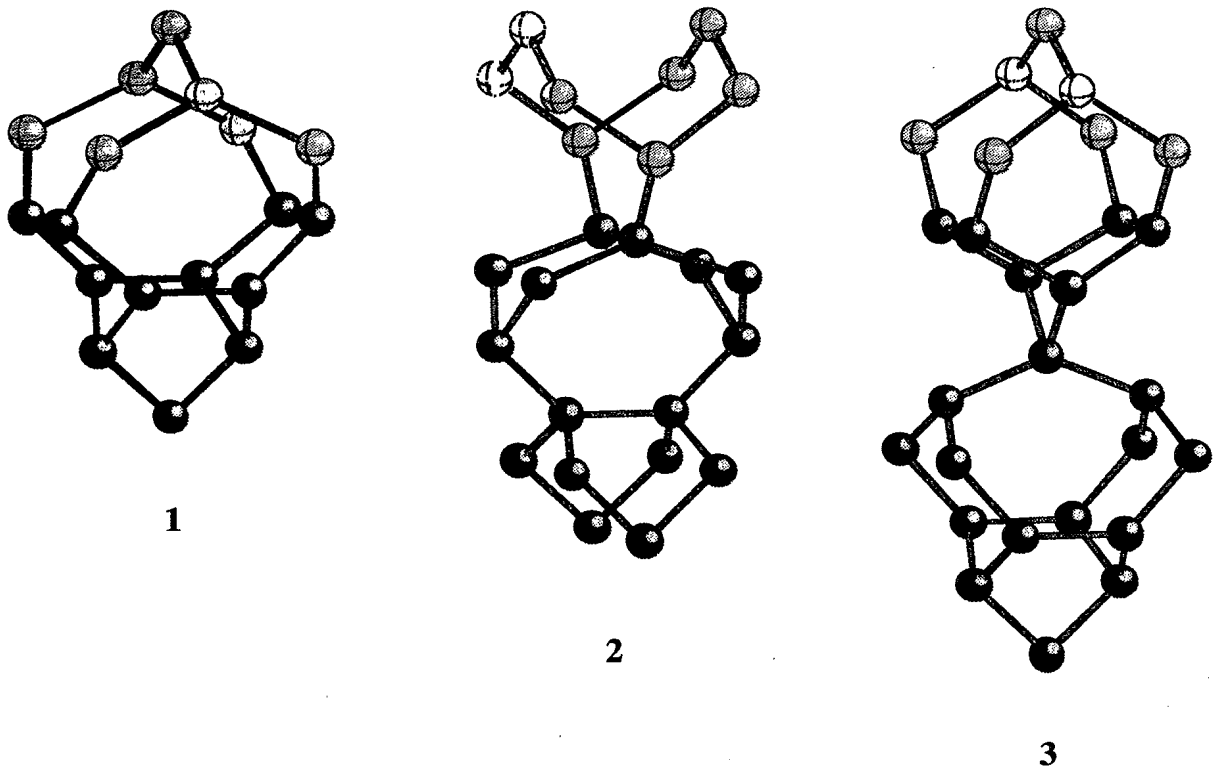

FIG. 2. The calculated structures of $(a/2)\langle 110\rangle$ edge dislocation intersections in Ge/Si(001) bicrystals for 1-, 3-, and 5-layer offsets along [0,0,1].

TABLE I. Energies (eV) for the relaxed samples with different numbers of atoms. V(Ge,Si) are total energies for all of the Ge,Si atoms in each bicrystal, and $V=V(\text{Ge})+V(\text{Si})$ is the total. $\langle E(\text{Ge,Si})\rangle$ are the average energies of the fourfold coordinated atoms of each type (atoms in the bottom and top surface layers are not included). $\langle\langle E(\text{Ge,Si})\rangle\rangle$ are averages across the four samples. For reference, E_{bulk}(Ge,Si) are the cohesive energy values in the pure bulk materials.

Intersection	Ge	Si	Total	V	V(Ge) $\langle E(\text{Ge})\rangle$	V(Si) $E(\text{Si})\rangle$
SW			$E_{\text{bulk}}(\text{Ge})=-3.8496$ $E_{\text{bulk}}(\text{Si})=-4.3342$ $\langle\langle E(\text{Ge})\rangle\rangle=-3.8384$, $\langle\langle E(\text{Si})\rangle\rangle=-4.3002$			
1	9216	9975	19 191	−76 968.6	−34 761.3 −3.8371	−42 207.3 −4.3043
2		9925	19 141	−76 735.3	−34 774.1 −3.8386	−41 961.1 −4.3010
3		9875	19 091	−76 502.1	−34 777.5 −3.8390	−41 724.6 −4.2987
4		9825	19 041	−76 269.6	−34 779.2 −3.8390	−41 490.4 −4.2967
Tersoff			$E_{\text{bulk}}(\text{Ge})=3.8438$, $E_{\text{bulk}}(\text{Si})=-4.6294$ $\langle\langle E(\text{Ge})\rangle\rangle=-3.8386$, $\langle\langle E(\text{Si})\rangle\rangle=-4.5758$			
1	9216	9975	19 191	−79 811.4	−34 790.9 −3.8371	−45 020.5 −4.5804
2		9925	19 141	−79 563.6	−34 805.9 −3.8388	−44 757.7 −4.5769
3		9875	19 091	−79 315.1	−34 809.4 −3.8392	−44 505.7 −4.5743
4		9825	19 041	−79 067.2	−34 810.9 −3.8395	−44 256.2 −4.5721

TABLE II. Energies (eV) for "standard" samples with the same number of Si atoms as for the dreidl at the interface. Each sample has 19 191 atoms =9216 Ge + 9975 Si. ΔV is the difference of the total energy from that for intersection 1.

Intersection	ΔV	V	V(Ge)	V(Si)
SW				
1		−76 968.6	−34 761.3	−42 207.3
2	18.3	−76 950.3	−34 774.1	−42 176.2
3	36.5	−76 932.1	−34 777.5	−42 154.7
4	53.9	−76 914.7	−34 779.2	−42 135.5
Tersoff				
1		−79 811.4	−34 790.9	−45 020.5
2	19.0	−79 792.4	−34 805.9	−44 986.5
3	38.8	−79 772.6	−34 809.4	−44 963.2
4	57.9	−79 753.5	−34 810.9	−44 942.6

TABLE III. The largest percentage changes in bond lengths, bond angles, and energies relative to the perfect crystals for atoms in the three intersections and in the core of the individual edge dislocations five to six layers away from the intersections.

Intersection	Bonds		Angles		Energies
SW					
1	−4.4	8.7	−12.9	23.9	8.8
2	−3.6	7.8	−14.7	22.7	6.8
3	−3.1	7.6	−17.1	23.2	6.3
individual	−2.7	7.0	−13.8	19.7	4.4
Tersoff					
1	−4.0	10.4	−14.2	24.3	10.7
2	−3.1	9.3	−17.3	23.3	7.3
3	−2.6	8.7	−19.8	22.5	9.4
individual	−2.1	7.8	−16.8	19.1	5.6

adding the appropriate multiple of $50\langle\langle E(\mathrm{Si})\rangle\rangle$ to the results for the other intersections. The results are given in Table II. It is apparent that the most compact intersection, the dreidl, is energetically preferred. This point is made clearly in the second column (ΔV) in Table II, which shows energy differences of the other intersections from intersection 1. Note that as the dislocation separation is increased in the 32-layer bicrystal, the strength of the interaction of the dislocation that is mostly in Si with its image reflected across the dimerized surface increases. Despite this surface interaction which favors separation, the more compact dreidl structure is favored by ~20 eV over intersection 2, and by ~55 eV compared to intersection 4 (no intersection). The results are independent of the potential used. While the dreidl is energeticaly preferred, the other intersections shown in Fig. 2 are (local) minimum energy configurations that may be observed as metastable states. It may be necessary for the interaction structure to change during the motion of one dislocation relative to the other, although we have not tried to simulate such climb. In addition, impurity segregation may have an effect on the relative stability of the intersection structures.

The largest changes in bond lengths, bond angles, and energies for the various intersections are summarized in Table III. The largest changes in bond lengths and energies generally diminish as the dislocations separate. For intersection 3, the atom with the largest strain energy is the single one shared by the two dislocations. The angular changes show that smaller angles occur as the offset between the dislocations increases.

In conclusion, we have used classical numerical simulations in large microcrystals of ~20 000 atoms to predict the structures and energies of intersections of $(a/2)\langle 110\rangle$ edge dislocations in diamond cubic crystals. The most compact of the three intersections is preferred. Photoluminescence experiments offer one possible way to look for and characterize these intersections. Electronic structure calculations to explore this possibility are planned if the very large computer resources needed can be obtained.

ACKNOWLEDGMENTS

The authors are grateful to Victor Milman for civilized conversations. Oak Ridge National Laboratory is operated for the U.S. Department of Energy by Martin Marietta Energy Systems, Inc., under Contract No. DE-AC05-84OR21400.

[1]M. Mostoller, M. F. Chisholm, and T. Kaplan, Phys. Rev. Lett. **72**, 1494 (1994).

[2]M. F. Chisholm, S. J. Pennycook, and D. E. Jesson, in *In-situ Patterning: Selective Area Deposition and Etching,* edited by A. F. Bernhardt, J. G. Black, and R. Rosenberg, MRS Symposia Proceedings No. 158 (Materials Research Society, Pittsburgh, 1990), p. 447.

[3]Dreidl (rhymes with cradle): a four-sided toy marked with Hebrew letters and spun like a top in a game of chance [Webster's Ninth New Collegiate Dictionary (Merriam Webster, Springfield, 1989)].

[4]J. Hornstra, J. Phys. Chem. Solids **5**, 129 (1958).

[5]A. S. Nandedkar and J. Narayan, Philos. Mag. A **56**, 625 (1987); **61**, 873 (1990).

[6]F. H. Stillinger and T. A. Weber, Phys. Rev. B **31**, 5262 (1985).

[7]K. Ding and C. Andersen, Phys. Rev. B **34**, 6987 (1987).

[8]M. Karimi, T. Kaplan, M. Mostoller, and D. E. Jesson, Phys. Rev. B **47**, 9931 (1993).

[9]J. Tersoff, Phys. Rev. B **39**, 5566 (1989).